

Fractal Quasicondensation in One Dimension

Flavio Riche,¹ Miguel Gonçalves,² Bruno Amorim,^{3,4} Eduardo V. Castro,^{5,6} and Pedro Ribeiro^{1,6}

¹*CeFEMA, LaPMET, Instituto Superior Técnico,*

Universidade de Lisboa, Av. Rovisco Pais, 1049-001 Lisboa, Portugal

²*Princeton Center for Theoretical Science, Princeton University, Princeton, NJ 08544*

³*Centro de Física das Universidades do Minho e Porto, LaPMET,
Universidade do Minho, Campus of Gualtar, 4710-057, Braga, Portugal*

⁴*International Iberian Nanotechnology Laboratory (INL),
Av. Mestre José Veiga, 4715-330 Braga, Portugal*

⁵*Centro de Física das Universidades do Minho e Porto, LaPMET,
Departamento de Física e Astronomia, Faculdade de Ciências,*

Universidade do Porto, 4169-007 Porto, Portugal

⁶*Beijing Computational Science Research Center, Beijing 100084, China*

We unveil a novel mechanism for quasicondensation of hard-core bosons in the presence of quasiperiodicity-induced multifractal single-particle states. The new critical state, here dubbed fractal quasicondensate, is characterized by natural orbitals with multifractal properties and by an occupancy of the lowest natural orbital, $\lambda_0 \simeq L^\gamma$, which grows with system size but with a non-universal scaling exponent, $\gamma < 1/2$. In contrast to fractal quasicondensates obtained when the chemical potential lies in a region of multifractal single-particle states, placing the chemical potential in regions of localized or delocalized states yields, respectively, no condensation or the usual 1D quasicondensation with $\gamma = 1/2$. Our findings are established by studying one-dimensional hard-core bosons subjected to various quasiperiodic potentials, including the well-known Aubry-André model, employing a mapping to non-interacting fermions that allows for numerically exact results. We discuss how to test our findings in state-of-the-art ultracold atom experiments.

I. INTRODUCTION

The localization of single-particle wave functions predicted by Anderson [4] can be induced by uncorrelated disorder or by quasiperiodic (QP) perturbations incommensurate with the underlying crystal. Quasiperiodicity can induce localization-delocalization transitions even in one dimension [5], where any finite amount of uncorrelated disorder immediately localizes the wave function [1, 10, 35, 40]. QP modulations may also lead to critical states with multifractal properties [19, 20, 22, 26, 38]. Such critical states arise at localization phase transitions and were also shown to ensue in extended areas of the phase space, where they can coexist with localized and extended states, albeit separated by the so-called mobility edges into different spectral regions [6, 13, 21, 45, 59].

Interest in QP single-particle systems, kickstarted in the 80's by the celebrated Aubry-André (AA) model [5], has been renewed by the possibility of engineering QP modulations in arrays of trapped atoms, cavity polaritons, and photonic lattices [2, 33, 34, 38, 53, 55, 64] and by the emergence of moiré systems, such as twisted bilayer graphene [24, 62].

In the presence of interactions, the effects of the interplay between quasiperiodicity and strong interactions is a subject under active investigation [23, 25, 57]. For one, it is yet unclear if electron-electron interactions and quasiperiodicity combined can explain the physics of twisted bilayer graphene [7, 8, 24].

In interacting bosonic systems, the Bose condensed state may also be affected by QP modulations [15, 41,

48, 50]. Its effects can even be observed in one dimension, where a macroscopic occupation of the condensed state is not possible and, instead, the superfluid phase is characterized by an occupation of the most populated state that grows as the square root of the total number of bosons [47]. This so-called quasicondensed state can be destroyed by a QP perturbation yielding a compressible insulating phase dubbed Bose glass [11, 14, 16, 37, 49, 63, 64]. In the strongly-coupling limit, where repulsive on-site interactions render bosons effectively hard-core particles, these effects have been well-established thanks to the Jordan-Wigner (JW) mapping onto non-interacting fermions [46]. As a result, a numerically exact analysis may be conducted for relatively large system sizes [37, 45, 58]. This has permitted to show that, when submitted to a QP potential, hard-core boson (HCB) lattices, host quasicondensed, Mott insulating or Bose glass phases, depending on the location of the chemical potential μ [45]. If μ lies in a spectral region where JW single-particle states are delocalized (localized), the system is a quasicondensate (Bose glass), and the fraction of particles in the most occupied state, λ_0 , behaves as $N_b^{1/2}$ (N_b^0), with N_b the total number of bosons. If μ lies in a spectral gap the system is a Mott insulator with $\lambda_0 \sim N_b^0$. The behavior of HCB in the AA model at criticality, including quantum dynamics analysis, was studied by He et al. [30, 31] and Gramsch et al. [27]. Nevertheless, the extension of such analysis to generalized AA models and the study of the multifractal localization properties of HCB critical states remains open.

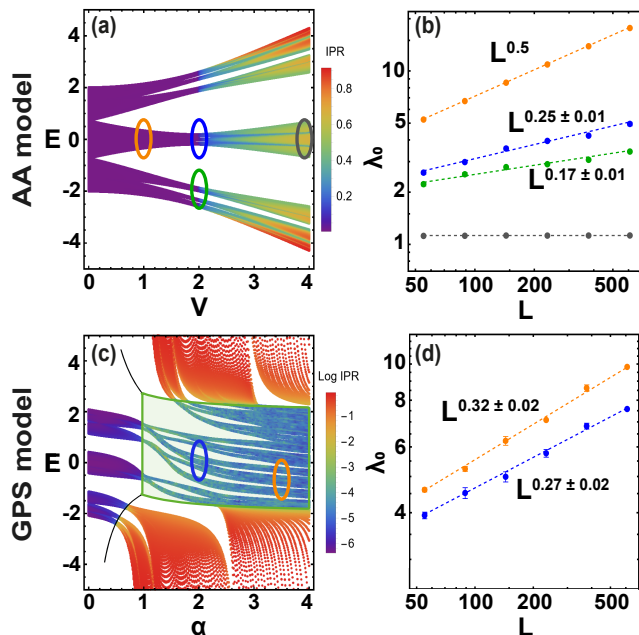


FIG. 1. **AA model.** (a) Fermionic IPR for the single-particle eigenstates as a function of the quasiperiodic potential strength, V , and energy, E , for system size $L = 610$. (b) Scaling of the natural orbital's highest eigenvalue, λ_0 , as a function of L for delocalized ($V = 1$, orange), critical ($V = 2$, blue), and localized ($V = 4$, gray) states at filling fraction $\nu = 1/2$. We also plot the scaling of critical states for $V = 2$ at $\nu = 0.29$ (green) to show that Bose superfluidity occurs for other filling fractions than $\nu = 1/2$. **GPS model.** (c) IPR of the JW fermions as a function of α and E , computed for $V = 0.75$ and $L = 610$. Black curves indicate extended-localized transitions. Critical phase is shaded in green. (d) Scaling of λ_0 with L for $\alpha = 2$ at $\nu = 0.48$ ($\alpha = 3.5$ at $\nu = 0.368$), where blue (orange) points are numerical results fitted by the dashed lines. Fractal quasicondensation is revealed by the sub-linear scalings $\lambda_0 \propto L^\gamma$ with $0 < \gamma < 1/2$. Results in (b,d) are averaged over 10 random configurations of θ and ϕ . Error bars are obtained from the standard deviation of the configurational average.

Here, we investigate the fate of the quasicondensed state when the chemical potential lies within a spectral region of fractal single-particle eigenstates arising at localization-delocalization transitions or in extended phase-space regions of critical states [3, 19, 38]. We show that critical 1D HCB are fractal quasicondensates, characterized by fractional occupation $\lambda_0 \sim N_b^\gamma$, with $0 < \gamma < 1/2$, and that the quasicondensed state exhibits multifractal localization properties. In the critical regime, the scaling exponent, γ , was found to be non-universal. To illustrate our findings we consider the AA model at criticality, and the Ganeshan-Pixley-Sarma (GPS) model [19] having anomalous mobility edges. Some of these results are summarized in Fig. 1, where we also show the single-particle inverse participation ratio (IPR) throughout the phase diagram of the AA and GPS models.

In the remainder of this article, we present the models and detail our analysis of the occupations and of the properties of the fractal quasicondensed state, we discuss our findings, and how our results may be observed experimentally. Additional data corroborating our conclusions and a discussion on particular implementations are provided in the Appendices.

II. MODEL AND METHODS

We consider N_b HCB on a 1D lattice with L sites and periodic boundary conditions. The Hamiltonian is given by:

$$H = - \sum_n (t b_n^\dagger b_{n+1} + \text{h.c.}) + \sum_n V_n^\gamma b_n^\dagger b_n, \quad (1)$$

where b_n (b_n^\dagger) is the bosonic annihilation (creation) operator at site $n = 1, \dots, L$. The hard-core limit imposes the constraints $b_n^2 = b_n^{\dagger 2} = 0$ and imply the same-site anti-commutation relation, $\{b_n, b_n^\dagger\} = 1$, in addition to the usual commutation relations, $[b_n, b_m^\dagger] = 0$, for $n \neq m$. t is the hopping integral and V_n^γ is the on-site incommensurate potential specified below (γ labels the two potentials considered). We apply twisted boundary conditions, i.e. $b_n^\dagger = b_{n+L}^\dagger e^{i\theta}$, with phase twists θ , that can be easily implemented through the Peierls substitution, $t \rightarrow t e^{i\theta/L}$. Subsequent numerical results are presented in units of t .

Concerning the QP potential, V_n^γ , the index $\gamma = \text{AA, GPS}$ labels the two considered models, with potentials respectively given by:

$$V_n^{\text{AA}} = V \cos(2\pi\tau n + \phi), \quad (2)$$

$$V_n^{\text{GPS}} = \frac{V \cos(2\pi\tau n + \phi)}{1 + \alpha \cos(2\pi\tau n + \phi)}. \quad (3)$$

The parameters (V , α), the phase shift ϕ , and τ , the ratio between the periods of the 1D lattice and the QP modulation, fully characterize the potential. We take τ to be the inverse of the Golden Ratio, $\tau = \varphi_R^{-1} = (\sqrt{5} - 1)/2$. For reducing finite-size effects, we consider rational approximants given by the ratio of two successive Fibonacci numbers, $\tau_j = F_{j-1}/F_j$, with $\tau = \tau_\infty$, and take $L = F_j$. We also average the numerical results over random boundary twists, θ , and shifts, ϕ , to further reduce finite-size effects.

For the AA model, transitions between delocalized ($0 < V < 2t$) and localized ($V > 2t$) states are energy independent and occur at $V_c = 2t$, as shown in Fig. 1(a). For the GPS model, the mobility edge is given by $E = (V \pm 2t)/\alpha$ [19], while the critical region is delimited by $|V - E\alpha| \leq |2t\alpha| \wedge |\alpha| \geq 1$ [38], as seen in Fig. 1(c).

After the JW mapping, $b_n^\dagger = c_n^\dagger \prod_{\beta=1}^{n-1} e^{-i\pi c_\beta^\dagger c_\beta}$, with c_n (c_n^\dagger) the fermionic annihilation (creation) operator, the fermionic Hamiltonian is given by Eq. (1), replacing b_n by c_n . The bosonic single-particle density matrix (SPDM), $\rho_{nm}^B = \langle b_m^\dagger b_n \rangle$, can be efficiently computed from its fermionic counterpart, $\rho_{nm}^F = \langle c_m^\dagger c_n \rangle$, computed by evaluating matrix determinants [46, 47]. Since the form of H remains unchanged after the JW mapping, both HCB and free fermions share the same energy spectrum. For diagonal entries $\rho_{nn}^B = \rho_{nn}^F$, thus differences between fermionic and bosonic single-particle density matrices are encoded in their off-diagonal correlations.

For homogeneous systems at zero temperature, quasicondensation is signaled by a divergence in the momentum distribution function at zero momentum $n_{\kappa=0} \sim \sqrt{N_b}$ [47]. The generalization for spatially inhomogeneous systems amounts to considering the highest eigenvalue of the bosonic SPDM, λ_0 . The eigenvectors of the SPDM, Φ_j^n , are called *natural orbitals* (NO), i.e. [36, 42, 46]:

$$\sum_j \rho_{ij}^B \Phi_j^n = \lambda_n \Phi_i^n, \quad (4)$$

with $\lambda_0 \geq \lambda_1 \geq \dots$. The number of bosons in the most occupied state scales with N_b , $\lambda_0 \sim (N_b)^\gamma$, with $\gamma = 0.5$ for quasicondensates associated with delocalized states and $\gamma = 0$ for Mott insulators and Bose Glasses.

In order to characterize phase transitions and analyze localization properties of the wavefunctions, we use the inverse participation ratio (IPR):

$$\text{IPR}[\psi] = \sum_n |\psi_n|^4, \quad (5)$$

where ψ is the normalized fermionic wavefunction. The IPR shows a power law scaling, $\text{IPR}[\psi] \sim L^{-\tau_F^R}$ (R stands for real space), with $\tau_F^R = 0$ for localized states, $\tau_F^R = d$ for extended states (d is the dimension) and $\tau_F^R = D_F$ for multifractal states (D_F is the fractal dimension, obeying $0 < D_F < d$) [18, 30, 38, 54]. The scaling analysis of the τ_F^R exponent shows that, for fermionic systems, the IPR of both extended and multifractal states tends to zero in the thermodynamic limit. Conversely, localization in momentum space can be quantified by the momentum space IPR (IPR_K) [43]:

$$\text{IPR}_K[\psi] = \sum_k |\tilde{\psi}_k|^4, \quad (6)$$

where $\tilde{\psi}_k$ are the Fourier coefficients of the wave function. $\text{IPR}_K[\psi] \sim L^{-\tau_F^K}$, with $\tau_F^K = d$ for localized and $\tau_F^K = 0$ for ballistic states. At criticality, both IPR and the IPR_K decrease with L . To study the localization properties of the bosonic systems, we consider $\text{IPR}[\Phi^n]$ and the $\text{IPR}_K[\Phi^n]$, with Φ^n the n -th NO.

III. RESULTS AND DISCUSSION

We start with the AA model, defined by Eq. (1) with the on-site potential in Eq. (2). For completeness, we show the single-particle results in Fig. 1(a), where the well-known energy-independent localization transition at $V_c = 2$ is clearly seen in the IPR values of the JW fermions. Figure 1(b) depicts the scaling of λ_0 with the system size at filling fraction ($\nu = N_b/L$) $\nu = 1/2$, for different values of V . For $V < V_c$ ($V > V_c$), the scaling $\lambda_0 \propto L^\gamma$ with $\gamma = 1/2$ ($\gamma = 0$) is recovered for the quasicondensed (Bose glass) state. At criticality ($V = V_c$), the AA model behaves as a Bose superfluid. For $\nu = 1/2$ (blue curve), the exponent $\gamma \simeq 0.25 \pm 0.01$ is obtained. Quasicondensation still occurs for $\nu \neq 1/2$, albeit with a smaller value for γ . The green curve in Fig. 1(b) shows the results at criticality for $\nu = 0.29$, where the corresponding scaling exponent is given by $\gamma \simeq 0.17 \pm 0.01$. Our results are in accordance with He et al. [31].

Now we turn to the GPS model, given by Eq. (1) with the incommensurate potential of Eq. (3). Figure 1(c) shows the density plot of the single-particle fermionic IPR as a function of the energy and of the parameter α . For $\alpha < 1$, only extended-localized transitions are observed. Transitions between critical-extended and critical-localized states occur at $\alpha = 1$ and $\alpha > 1$, respectively.

Figure 1(d) shows the scaling of λ_0 , for two values of the parameters (α, ν) in the critical region indicated in Fig. 1(c). As for the AA model, we find $0 < \gamma < 1/2$, indicating the presence of an exotic quasicondensed state. Specifically, we obtain $\gamma = 0.27 \pm 0.02$ and $\gamma = 0.32 \pm 0.02$ for $(\alpha, \nu) = (2, 0.48)$ and $(\alpha, \nu) = (3.5, 0.368)$, respectively. We attribute the different scaling exponents to the parameter-dependent fractal properties of the single-particle states [32, 54, 56] which manifest in the bosonic NO through an exotic type of quasicondensation, here dubbed fractal quasicondensation, with a tunable scaling exponent γ . It should be noted that even for a model without energy-dependent mobility edges, such as the AA model, such scaling exponent can be tuned by means of the filling fraction.

To investigate the fractal nature of the lowest NO (i.e. $\Phi^{n=0}$) at criticality, we compute the scaling of their IPR and IPR_K , as defined by Eqs. (5) and (6), respectively. The results are compared with the scalings of the fermionic single-particle eigenstates at the same filling. This analysis is made for the AA model at $V = 2$ in Fig. 2(a,b), and for the GPS model in Fig. 2(c,d).

Fig. 2(a) shows that since $0 < \tau_B^R < 1$ ($\tau_B^R = 0.84 \pm 0.02$), the lowest NO is fractal albeit much more delocalized in real space than its fermionic counterpart ($\tau_F = 0.61 \pm 0.01$). Concomitantly, the analysis of the IPR_K in Fig. 2(b) yields $\tau_F^K = 0.62 \pm 0.01$, $\tau_B^K = 0.05 \pm 0.01$, and indicates that the lowest NO is very localized in mo-

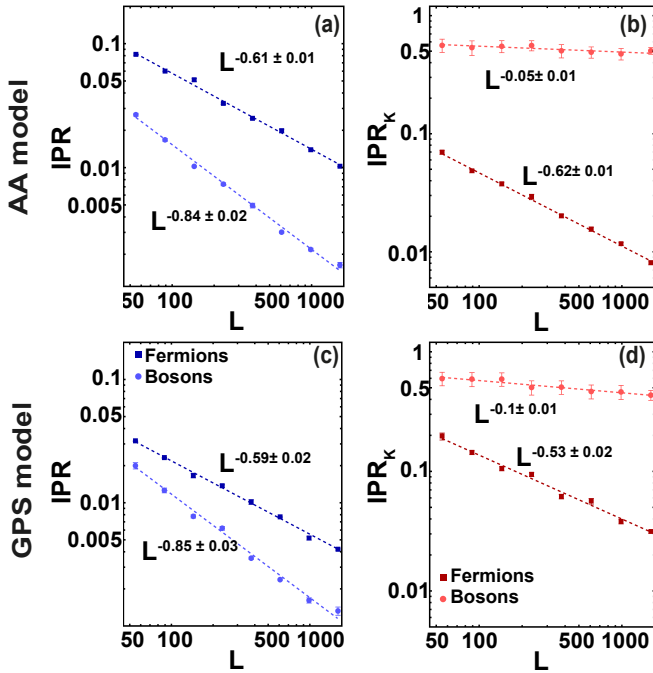


FIG. 2. **AA model** ($V = 2$). (a) IPR scaling of the fermionic eigenvectors (natural orbitals), indicated by dark (light) blue points with error bars, where the dark (light) red curve corresponds to the fitted model $\text{IPR} \sim L^{-\tau_{F(B)}^R}$, with the exponent $\tau_F^R = 0.61 \pm 0.01$ ($\tau_B^R = 0.84 \pm 0.02$). (b) IPR_K scaling of the fermionic eigenvectors (natural orbitals), indicated by dark (light) red points. The IPR_K of the fermionic eigenvectors scales as $\text{IPR}_K \sim L^{-\tau_F^K}$, with $\tau_F^K = 0.62 \pm 0.01$ ($\tau_B^K = 0.05 \pm 0.01$). **GPS model** ($V = 0.75$, $\alpha = 3.5$, $\nu = 0.368$). (c) IPR scaling of the fermionic eigenvectors (natural orbitals), indicated by dark (light) blue points, where the dark (light) curve is a fit yielding the the exponent $\tau_F^R = 0.59 \pm 0.02$ ($\tau_B^R = 0.85 \pm 0.03$). (d) IPR_K scaling of the fermionic eigenvectors (natural orbitals), indicated by dark (light) red points, with $\tau_F^K = 0.53 \pm 0.02$ ($\tau_B^K = 0.1 \pm 0.01$). Results are averaged over 30 random configurations of θ and ϕ .

mentum space and thus is much closer to a plane wave than the fermionic wave-function. Together these results suggest a weak fractal nature of the NO. In the following, we show that this is due to strong finite-size effects and that the scaling exponents at criticality are fractal-like.

Despite the disparities between the scaling exponents of the bosonic and fermionic models, the localization transition occurs for the same critical potential $V_c = 2$ in both models. This is analyzed in Fig. 3(a) which displays the IPR (IPR_K) of the NO as a function of the potential V , for different system sizes. For small (high) V , the IPR (IPR_K) of the NO decreases with L , whereas for high (small) V , the IPR (IPR_K) becomes L -independent. As a result, at the transition point, these quantities cross in the thermodynamic limit. However, Fig. 3(b), show that the finite L crossing point has prominent finite-size effects, which are much less severe in the fermionic case,

but are nevertheless compatible with $V_c = 2$. At the same point, the critical exponents of the IPR and IPR_K estimated by extrapolating the finite-size crossing point values, see Fig. 3(c), yields $\tau_B^R = \tau_B^K \sim 0.52$ which clearly established the fractal nature of the lowest NO. Thus, the exponents naively obtained in Fig. 2(a) and (b) that point to a weak fractal nature of the NO are a consequence of the strong finite size effects.

To further study the fractal nature of the NO, in particular its multifractality content, we consider the q -generalization of IPR [18, 52] defined as:

$$\text{IPR}_{R/K}(q) = \sum_{\tau/k} |\psi_{\tau/k}|^{2q} \sim L^{-\tau^{R/K}(q)}, \quad (7)$$

and analyze its behavior at the the crossing point in Fig. 3(d). The onset of multifractality corresponds to a non-linearity dependence of the exponent $\tau^{R/K}$ with q [18, 52].

For free fermions, we verify that $\tau_F^R(q) = \tau_F^K(q)$ for all q as required by the self-duality of the AA model at $V = V_c$. For HCBs, although the transition still arises for the same value of V , the position and momentum space natural orbitals are no longer self-dual. Interestingly, in this case, we observe strong finite size effects at the critical point. Nevertheless, we still observe a non-linear dependence of both $\tau_B^R(q)$ and $\tau_B^K(q)$ with q , signaling a the multifractal nature of the lowest NO.

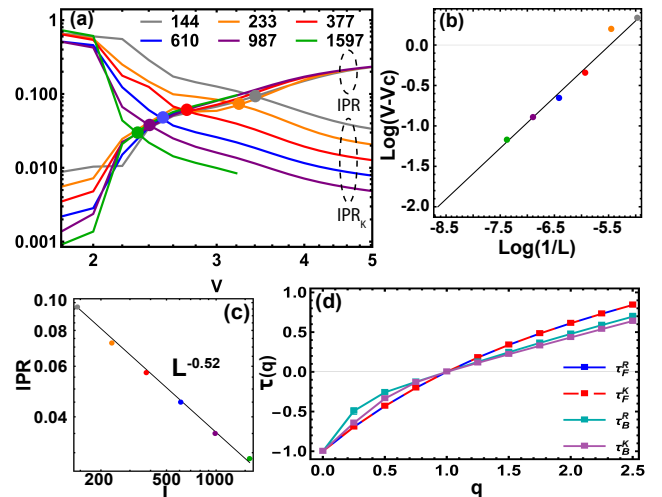


FIG. 3. **AA model**. (a) IPR and IPR_K of the NOs versus the on-site potential (V) for various values of L . (b) Extrapolation of the logarithm of the drift from the critical point versus $\log(1/L)$, showing that the finite-size scaling is compatible with $V_c = 2$. (c) Scaling of IPR and IPR_K for the lowest NO computed at the crossing point of (a). (d) Scaling exponents $\tau_{F(B)}^{R/K}(q)$ versus the scaling parameter q , for free fermions (HCBs) in position, τ_F^R (τ_B^R), and momentum, τ_F^K (τ_B^K), spaces as an indicator of multifractality.

IV. EXPERIMENTAL IMPLEMENTATION

In this section we argue that the mechanism of quasi-condensation we propose can be probed in current state-of-the-art experiments with cold atomic gases. To avoid having to tune the system to a critical point, we focus on the GPS model for which multifractal states occupy a finite region of the phase diagram. However, the implementation of the QP potential described in Eq. (3) may be challenging, due its unbounded nature for $\alpha \geq 1$. To overcome this obstacle, we can resort to the *Floquet engineered Hamiltonian* proposed by [17, 29, 39] given by:

$$H = - \sum_n (tb_n^\dagger b_{n+1} + \text{h.c.}) + \sum_n \frac{V}{1 + \alpha \cos(2\pi\tau n + \phi)} b_n^\dagger b_n. \quad (8)$$

As depicted in Fig. 4(a), this simplified family of models still possesses a region of critical states that is shown to host quasicondensed states in Fig. 4(b). These models were shown to be physically realizable with conventional optical lattice techniques by Liu et al.[38] for the fermionic case. As in previous works [9, 12, 28, 44, 51, 60, 61], the adaptation of this method to HCB can be achieved by tuning the Feshbach resonances as to make the interaction strength much higher than any other energy scale, thus enforcing the hard-core constraint. The critical nature of the states both in momentum and real space can be inferred from time-of-flight experiments[14] and from direct measurements of the populations by absorption imaging[2]. Further details on the implementation of unbounded potentials using Floquet engineered Hamiltonians are given in Appendix B.

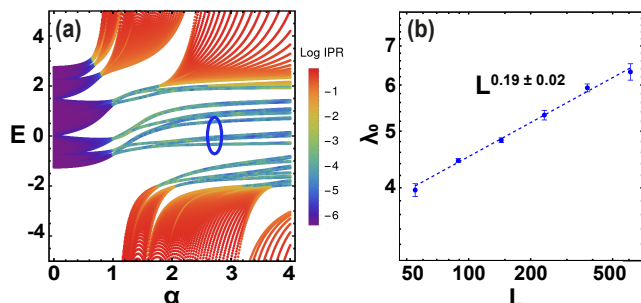


FIG. 4. **Simplified version of the GPS model.** (a) Density plot of the IPR as a function of the energy and of the on-site potential, for $L = 610$. (b) Scaling of the natural orbital's highest eigenvalue (λ_0) at the critical point, for $(\nu, \alpha) = (0.49, 2.75)$. (b) The quasicondensation revealed by the scaling of the occupation of the lowest NO, $\gamma_0 \sim L^\gamma$ with $\gamma < 1/2$.

V. CONCLUSIONS

In this article, we study the condensation of HCB in the presence of quasiperiodic-induced critical states with multifractal wavefunctions. We show that when the chemical potential is placed in regions where the single-particle state are critical, quasicondensation acquires exotic features. This regime, dubbed fractal quasicondensation, is characterized by the growth of the occupation of the lowest natural orbital, albeit with an exponent smaller than the value $\nu = 1/2$ that is observed in one-dimension quasicondensates with ballistic single-particle states. We analyze the real and momentum space structure of the lowest NO and reveal its multifractal nature.

Finally, we propose how to implement such a generalized AA model that hosts quasicondensed states. We hope our work sparks interest in the observation and further exploration of these novel fractal quasicondensed states, and leads to new insights in the interplay of strong interactions and quasiperiodicity.

ACKNOWLEDGEMENTS

The authors MG and PR acknowledge partial support from Fundação para a Ciência e Tecnologia (FCT-Portugal) through Grant No. UID/CTM/04540/2019. FR, MG and PR acknowledge support by FCT through Grant No. UIDB/04540/2020. BA and EVC acknowledge partial support from FCT-Portugal through Grant No. UIDB/04650/2020. MG acknowledges further support from FCT-Portugal through the Grant SFRH/BD/145152/2019. BA acknowledges further support from FCT-Portugal through Grant No. CEECIND/02936/2017.

APPENDIX A: ADDITIONAL RESULTS FOR THE GPS MODEL AT CRITICALITY

For completeness, we also show the results of the IPR scalings for the fermionic vectors and for the natural orbitals (NOs) of another phase-space state of the GPS model, with $V = 0.75$, $\alpha = 2$, $\nu = 0.48$. The results are similar to those obtained in the main article, depicted in Figs. 2(c,d). As we can see in Fig. A1, the scaling exponent of the fermionic eigenvectors is less than one for the IPR both in position and in momentum space. For the natural orbitals, due to the finite-size effects discussed in the main text, the IPR_K decreases very slowly, with a scaling exponent close to Fig. 2(d).

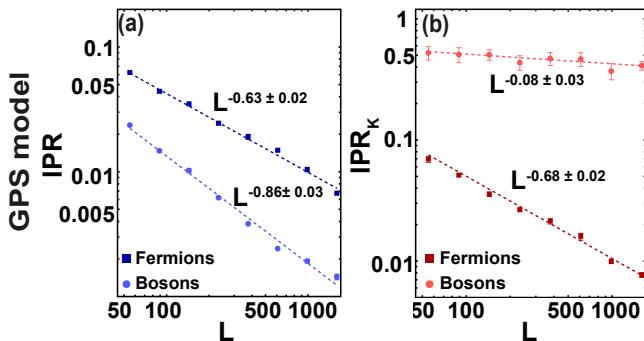


FIG. A1. **GPS Model.** IPR and IPR_K analysis inside the critical phase region ($V = 0.75$, $\alpha = 2$, $\nu = 0.48$). (a) IPR scaling of the fermionic eigenvectors (bosonic natural orbitals), indicated by dark (light) blue points, where the dark (light) curve corresponds to the fitting, with the scaling exponent $\tau_F^R = 0.63 \pm 0.02$ ($\tau_B^R = 0.86 \pm 0.03$). (b) IPR_K scaling of the fermionic eigenvectors (bosonic natural orbitals), indicated by dark (light) red points, with the exponent $\tau_F^K = 0.68 \pm 0.02$ ($\tau_B^K = 0.08 \pm 0.03$). The results were averaged over 30 random configurations of twists θ and phases ϕ .

APPENDIX B: FLOQUET ENGINEERED HAMILTONIANS AND THE IMPLEMENTATION OF UNBOUNDED POTENTIALS

In this section, we discuss in more details how to overcome problems related with the physical implementation of the GPS model in order to probe fractal quasicondensation. As mentioned in Section IV, *Floquet engineered Hamiltonians* are an effective way to overcome the potential divergences associated with unbounded potentials such as those of Eq. 3. Here we show how to map the Floquet eigenvalue equation onto the following tight-binding equation:

$$H = -t \sum_x (c_x^\dagger c_{x+1} + \text{h.c.}) + \sum_x \frac{V}{1 + \alpha \cos(2\pi\tau x + \phi)} c_x^\dagger c_x. \quad (\text{B1})$$

Although this Hamiltonian is different form that of the GPS model, given in Eq. 3, we show below it yields the same qualitative features, namely an extended critical phase. To implement this Hamiltonian, we follow the approach of Ref. [38] starting from a periodically-kicked quantum 1D system, described by the Schrödinger equation (in units where $\hbar = 1$):

$$K(p) \sum_n \delta(t - nT) |X, t\rangle + V(x) |X, t\rangle = i \partial_t |X, t\rangle. \quad (\text{B2})$$

The advantage of kicking the kinetic term, instead of the more common approach where the potential term is engineered, is that we can recover Eq. B1 in position space. This is particularly relevant for ensuring the hard-

core constraint. The evolution of the wavefunction for one kick is given by:

$$e^{-i \sum_x V_x c_x^\dagger c_x} e^{-i \sum_p K_p c_p^\dagger c_p} |x, t = m\rangle = |x, t = m + 1\rangle, \quad (\text{B3})$$

where $V(x) = \sum_x V_x c_x^\dagger c_x$ and $K(p) = \sum_p K_p c_p^\dagger c_p$. By defining $|X, t = m\rangle \equiv |X\rangle e^{-i\mu m}$, where $-\pi \leq \mu \leq \pi$ is the Floquet quasi-energy, we can rewrite Eq. (B3) in terms of an eigenvalue problem:

$$e^{-i \sum_x V_x c_x^\dagger c_x} e^{-i \sum_p K_p c_p^\dagger c_p} |X\rangle = e^{-i\mu} |X\rangle. \quad (\text{B4})$$

The next step is to introduce the auxiliary operator, $W(p) \equiv \tan\left(\frac{\sum_p K_p c_p^\dagger c_p}{2}\right)$, which gives:

$$e^{-i \sum_p K_p c_p^\dagger c_p} = \frac{1 - iW(p)}{1 + iW(p)}. \quad (\text{B5})$$

We also define:

$$|X\rangle \equiv [1 + iW(p)]|x\rangle. \quad (\text{B6})$$

Eqs. (B5) and (B6) in Eq. (B4) yields:

$$[1 + iW(p)]|x\rangle = e^{i\mu - i \sum_x V_x c_x^\dagger c_x} [1 - iW(p)]|x\rangle, \quad (\text{B7})$$

which can be rewritten as:

$$W(p)|x\rangle = S_x|x\rangle, \quad (\text{B8})$$

where $\frac{1+iS_x}{1-iS_x} = e^{i\mu - i \sum_x V_x c_x^\dagger c_x}$. Also:

$$W(p) = \sum_p W_p c_p^\dagger c_p |p\rangle \langle p| = \sum_{x,x'} |x\rangle W_{x-x'} \langle x'|, \quad (\text{B9})$$

and from Eq. (B9) in (B8):

$$\sum_{x,x'} |x\rangle W_{x-x'} \langle x'|x\rangle = S_x|x\rangle. \quad (\text{B10})$$

Now we show how to recover the tight-binding model of Eq. (B1), starting from the left-hand side of Eq. (B10), from which we are going to derive the hopping terms. Since $K(p) = \sum_p K_p c_p^\dagger c_p$ is diagonal in Bloch basis, with energies $\varepsilon_p = -2t \cos(p)$, we can write the auxiliary operator as:

$$W(p) = \tan\left(\frac{\varepsilon_p}{2}\right) \sim \frac{\varepsilon_p}{2} = -t \cos(p), \quad (\text{B11})$$

since the kick time is much smaller than the inter-kick time, $\tau \ll T$. Considering only first neighbors, Eq. (B10) reads:

$$-t|x-1\rangle - t|x+1\rangle = S_x|x\rangle. \quad (\text{B12})$$

The right-hand side of Eq. (B8) will give us the QP potential and the eigenvalues based on the Floquet quasi-energy. By defining $E \equiv 1/\tan(\mu/2)$ and rewriting $\frac{1+iS_x}{1-iS_x} = e^{i\mu-i\sum_x V_x c_x^\dagger c_x}$ we obtain

$$S_x = E - \sum_x \frac{V}{1 + \frac{1}{E} \tan\left(\frac{V_x}{2}\right)} c_x^\dagger c_x, \quad (\text{B13})$$

where $V \equiv \frac{1+E^2}{E}$.

To recover Eq. (B1) we set $V_x = 2 \arctan[A \cos(2\pi\tau x + \phi)]$. The QP potential in Eq. (B13) becomes:

$$\sum_x \frac{V}{1 + \alpha \cos(2\pi\tau x + \phi)} c_x^\dagger c_x, \quad (\text{B14})$$

where $\alpha = A/E$, varying without divergences.

-
- [1] E. Abrahams, P. W. Anderson, D. C. Licciardello, and T. V. Ramakrishnan, “Scaling theory of localization: Absence of quantum diffusion in two dimensions,” *Phys. Rev. Lett.*, vol. 42, pp. 673–676, Mar 1979. [Online]. Available: <https://link.aps.org/doi/10.1103/PhysRevLett.42.673>
- [2] F. A. An, K. Padavić, E. J. Meier, S. Hegde, S. Ganeshan, J. H. Pixley, S. Vishveshwara, and B. Gadway, “Interactions and Mobility Edges: Observing the Generalized Aubry-André Model,” *Physical Review Letters*, vol. 126, no. 4, p. 040603, jan 2021. [Online]. Available: <https://link.aps.org/doi/10.1103/PhysRevLett.126.040603>
- [3] F. A. An, K. Padavić, E. J. Meier, S. Hegde, S. Ganeshan, J. Pixley, S. Vishveshwara, and B. Gadway, “Interactions and mobility edges: Observing the generalized aubry-andré model,” *Physical review letters*, vol. 126, no. 4, p. 040603, 2021.
- [4] P. W. Anderson, “Absence of diffusion in certain random lattices,” *Physical review*, vol. 109, no. 5, p. 1492, 1958.
- [5] S. Aubry and G. André, “Analyticity breaking and anderson localization in incommensurate lattices,” *Ann. Israel Phys. Soc.*, vol. 3, no. 133, p. 18, 1980.
- [6] J. Biddle, D. Priour Jr, B. Wang, and S. D. Sarma, “Localization in one-dimensional lattices with non-nearest-neighbor hopping: Generalized anderson and aubry-andré models,” *Physical Review B*, vol. 83, no. 7, p. 075105, 2011.
- [7] Y. Cao, V. Fatemi, A. Demir, S. Fang, S. L. Tomarken, J. Y. Luo, J. D. Sanchez-Yamagishi, K. Watanabe, T. Taniguchi, E. Kaxiras *et al.*, “Correlated insulator behaviour at half-filling in magic-angle graphene superlattices,” *Nature*, vol. 556, no. 7699, pp. 80–84, 2018.
- [8] Y. Cao, V. Fatemi, S. Fang, K. Watanabe, T. Taniguchi, E. Kaxiras, and P. Jarillo-Herrero, “Unconventional superconductivity in magic-angle graphene superlattices,” *Nature*, vol. 556, no. 7699, pp. 43–50, 2018.
- [9] C. Chin, R. Grimm, P. Julienne, and E. Tiesinga, “Feshbach resonances in ultracold gases,” *Reviews of Modern Physics*, vol. 82, no. 2, p. 1225, 2010.
- [10] M. Continentino, *Quantum scaling in many-body systems*. Cambridge University Press, 2017.
- [11] B. Damski, J. Zakrzewski, L. Santos, P. Zoller, and M. Lewenstein, “Atomic bose and anderson glasses in optical lattices,” *Physical review letters*, vol. 91, no. 8, p. 080403, 2003.
- [12] T.-S. Deng, W. Zhang, and W. Yi, “Tuning feshbach resonances in cold atomic gases with interchannel coupling,” *Physical Review A*, vol. 96, no. 5, p. 050701, 2017.
- [13] X. Deng, S. Ray, S. Sinha, G. Shlyapnikov, and L. Santos, “One-dimensional quasicrystals with power-law hopping,” *Physical review letters*, vol. 123, no. 2, p. 025301, 2019.
- [14] C. D’Errico, E. Lucioni, L. Tanzi, L. Gori, G. Roux, I. P. McCulloch, T. Giamarchi, M. Inguscio, and G. Modugno, “Observation of a disordered bosonic insulator from weak to strong interactions,” *Physical review letters*, vol. 113, no. 9, p. 095301, 2014.
- [15] Y. Eksioglu, P. Vignolo, and M. Tosi, “Matter-wave interferometry in periodic and quasi-periodic arrays,” *Optics communications*, vol. 243, no. 1-6, pp. 175–181, 2004.
- [16] L. Fallani, J. Lye, V. Guarrera, C. Fort, and M. Inguscio, “Ultracold atoms in a disordered crystal of light: Towards a bose glass,” *Physical review letters*, vol. 98, no. 13, p. 130404, 2007.
- [17] S. Fishman, D. Grempel, and R. Prange, “Chaos, quantum recurrences, and anderson localization,” *Physical Review Letters*, vol. 49, no. 8, p. 509, 1982.
- [18] Y. Fu, E. J. König, J. H. Wilson, Y.-Z. Chou, and J. H. Pixley, “Magic-angle semimetals,” *npj Quantum Materials*, vol. 5, no. 1, pp. 1–8, 2020.
- [19] S. Ganeshan, J. Pixley, and S. D. Sarma, “Nearest neighbor tight binding models with an exact mobility edge in one dimension,” *Physical review letters*, vol. 114, no. 14, p. 146601, 2015.
- [20] M. Gonçalves, B. Amorim, E. Castro, and P. Ribeiro, “Hidden dualities in 1D quasiperiodic lattice models,” *SciPost Physics*, vol. 13, no. 3, p. 046, sep 2022. [Online]. Available: <https://scipost.org/10.21468/SciPostPhys.13.3.046>
- [21] M. Gonçalves, B. Amorim, E. V. Castro, and P. Ribeiro, “Critical phase dualities in 1d exactly solvable quasiperiodic models,” *Physical Review Letters*, vol. 131, no. 18, p. 186303, 2023.
- [22] —, “Renormalization group theory of one-dimensional quasiperiodic lattice models with commensurate approximants,” *Physical Review B*, vol. 108, no. 10, p. L100201, sep 2023. [Online]. Available: <https://link.aps.org/doi/10.1103/PhysRevB.108.L100201>
- [23] M. Gonçalves, B. Amorim, F. Riche, E. V. Castro, and P. Ribeiro, “Incommensurability enabled quasi-fractal order in 1d narrow-band moiré systems,” *Nature Physics*, pp. 1–8, 2024.
- [24] M. Gonçalves, H. Z. Olyaei, B. Amorim, R. Mondaini, P. Ribeiro, and E. V. Castro, “Incommensurability-induced sub-ballistic narrow-band-states in twisted bilayer graphene,” *2D Materials*, vol. 9, no. 1, p. 011001, jan 2022. [Online]. Available: <https://iopscience.iop.org/article/10.1088/2053-1583/ac3259>
- [25] M. Gonçalves, J. H. Pixley, B. Amorim, E. V. Castro, and P. Ribeiro, “Short-range interactions are irrelevant at the

- quasiperiodicity-driven luttinger liquid to anderson glass transition,” *Physical Review B*, vol. 109, no. 1, p. 014211, 2024.
- [26] M. Gonçalves, P. Ribeiro, E. V. Castro, and M. A. Araújo, “Disorder-driven multifractality transition in weyl nodal loops,” *Physical Review Letters*, vol. 124, no. 13, p. 136405, 2020.
- [27] C. Gramsch and M. Rigol, “Quenches in a quasidisordered integrable lattice system: Dynamics and statistical description of observables after relaxation,” *Physical Review A*, vol. 86, no. 5, p. 053615, 2012.
- [28] M. Greiner, O. Mandel, T. Esslinger, T. W. Hänsch, and I. Bloch, “Quantum phase transition from a superfluid to a mott insulator in a gas of ultracold atoms,” *nature*, vol. 415, no. 6867, pp. 39–44, 2002.
- [29] D. Grempel, R. Prange, and S. Fishman, “Quantum dynamics of a nonintegrable system,” *Physical Review A*, vol. 29, no. 4, p. 1639, 1984.
- [30] K. He, L. F. Santos, T. M. Wright, and M. Rigol, “Single-particle and many-body analyses of a quasiperiodic integrable system after a quench,” *Physical Review A*, vol. 87, no. 6, p. 063637, 2013.
- [31] K. He, I. I. Satija, C. W. Clark, A. M. Rey, and M. Rigol, “Noise correlation scalings: Revisiting the quantum phase transition in incommensurate lattices with hard-core bosons,” *Physical Review A*, vol. 85, no. 1, p. 013617, 2012.
- [32] H. Hiramoto and M. Kohmoto, “Scaling analysis of quasiperiodic systems: Generalized harper model,” *Phys. Rev. B*, vol. 40, pp. 8225–8234, Oct 1989. [Online]. Available: <https://link.aps.org/doi/10.1103/PhysRevB.40.8225>
- [33] T. Kohler, S. Scherg, X. Li, H. P. Lüschen, S. D. Sarma, I. Bloch, and M. Aidelsburger, “Observation of many-body localization in a one-dimensional system with a single-particle mobility edge,” *Physical review letters*, vol. 122, no. 17, p. 170403, 2019.
- [34] Y. Lahini, R. Pugatch, F. Pozzi, M. Sorel, R. Morandotti, N. Davidson, and Y. Silberberg, “Observation of a localization transition in quasiperiodic photonic lattices,” *Physical review letters*, vol. 103, no. 1, p. 013901, 2009.
- [35] P. A. Lee and T. Ramakrishnan, “Disordered electronic systems,” *Reviews of Modern Physics*, vol. 57, no. 2, p. 287, 1985.
- [36] A. J. Leggett, “Bose-einstein condensation in the alkali gases: Some fundamental concepts,” *Reviews of Modern Physics*, vol. 73, no. 2, p. 307, 2001.
- [37] S. Lellouch and L. Sanchez-Palencia, “Localization transition in weakly interacting bose superfluids in one-dimensional quasiperiodic lattices,” *Physical Review A*, vol. 90, no. 6, p. 061602, 2014.
- [38] T. Liu, X. Xia, S. Longhi, and L. Sanchez-Palencia, “Anomalous mobility edges in one-dimensional quasiperiodic models,” *SciPost Physics*, vol. 12, no. 1, p. 027, 2022.
- [39] S. Longhi, “Maryland model in optical waveguide lattices,” *Optics Letters*, vol. 46, no. 3, pp. 637–640, 2021.
- [40] A. MacKinnon and B. Kramer, “One-parameter scaling of localization length and conductance in disordered systems,” *Phys. Rev. Lett.*, vol. 47, pp. 1546–1549, Nov 1981. [Online]. Available: <https://link.aps.org/doi/10.1103/PhysRevLett.47.1546>
- [41] M. Modugno, “Exponential localization in one-dimensional quasi-periodic optical lattices,” *New Journal of Physics*, vol. 11, no. 3, p. 033023, 2009.
- [42] O. Penrose and L. Onsager, “Bose-einstein condensation and liquid helium,” *Physical Review*, vol. 104, no. 3, p. 576, 1956.
- [43] J. Pixley, J. H. Wilson, D. A. Huse, and S. Gopalakrishnan, “Weyl semimetal to metal phase transitions driven by quasiperiodic potentials,” *Physical review letters*, vol. 120, no. 20, p. 207604, 2018.
- [44] S. Ray, M. Pandey, A. Ghosh, and S. Sinha, “Localization of weakly interacting bose gas in quasiperiodic potential,” *New Journal of Physics*, vol. 18, no. 1, p. 013013, 2015.
- [45] P. Ribeiro, M. Haque, and A. Lazarides, “Strongly interacting bosons in multichromatic potentials supporting mobility edges: Localization, quasi-condensation, and expansion dynamics,” *Physical Review A*, vol. 87, no. 4, p. 043635, 2013.
- [46] M. Rigol and A. Muramatsu, “Universal properties of hard-core bosons confined on one-dimensional lattices,” *Physical Review A*, vol. 70, no. 3, p. 031603, 2004.
- [47] M. A. Rigol and A. Muramatsu, “Hard-core bosons and spinless fermions trapped on 1d lattices,” *Journal of low temperature physics*, vol. 138, no. 3-4, pp. 645–650, 2005.
- [48] G. Roati, C. D’Errico, L. Fallani, M. Fattori, C. Fort, M. Zaccanti, G. Modugno, M. Modugno, and M. Inguscio, “Anderson localization of a non-interacting bose-einstein condensate,” *Nature*, vol. 453, no. 7197, pp. 895–898, 2008.
- [49] R. Roth and K. Burnett, “Phase diagram of bosonic atoms in two-color superlattices,” *Physical Review A*, vol. 68, no. 2, p. 023604, 2003.
- [50] L. Sanchez-Palencia and L. Santos, “Bose-einstein condensates in optical quasicrystal lattices,” *Physical Review A*, vol. 72, no. 5, p. 053607, 2005.
- [51] M. Schreiber, S. S. Hodgman, P. Bordia, H. P. Lüschen, M. H. Fischer, R. Vosk, E. Altman, U. Schneider, and I. Bloch, “Observation of many-body localization of interacting fermions in a quasirandom optical lattice,” *Science*, vol. 349, no. 6250, pp. 842–845, 2015.
- [52] A. Siebesma and L. Pietronero, “Multifractal properties of wave functions for one-dimensional systems with an incommensurate potential,” *EPL (Europhysics Letters)*, vol. 4, no. 5, p. 597, 1987.
- [53] K. Singh, K. Saha, S. A. Parameswaran, and D. M. Weld, “Fibonacci optical lattices for tunable quantum quasicrystals,” *Physical Review A*, vol. 92, no. 6, p. 063426, 2015.
- [54] A. Szabó and U. Schneider, “Non-power-law universality in one-dimensional quasicrystals,” *Physical Review B*, vol. 98, no. 13, p. 134201, 2018.
- [55] D. Tanese, E. Gurevich, F. Baboux, T. Jacqmin, A. Lemaître, E. Galopin, I. Sagnes, A. Amo, J. Bloch, and E. Akkermans, “Fractal energy spectrum of a polariton gas in a fibonacci quasiperiodic potential,” *Physical review letters*, vol. 112, no. 14, p. 146404, 2014.
- [56] C. Tang and M. Kohmoto, “Global scaling properties of the spectrum for a quasiperiodic schrödinger equation,” *Phys. Rev. B*, vol. 34, pp. 2041–2044, Aug 1986. [Online]. Available: <https://link.aps.org/doi/10.1103/PhysRevB.34.2041>
- [57] D. Vu and S. D. Sarma, “Moiré versus mott: Incommensuration and interaction in one-dimensional bichromatic lattices,” *Physical Review Letters*, vol. 126, no. 3, p. 036803, 2021.
- [58] Y. Wang, C. Cheng, X.-J. Liu, and D. Yu, “Many-body critical phase: extended and nonthermal,” *Physical Re-*

- view Letters*, vol. 126, no. 8, p. 080602, 2021.
- [59] Y. Wang, X. Xia, L. Zhang, H. Yao, S. Chen, J. You, Q. Zhou, and X.-J. Liu, “One-dimensional quasiperiodic mosaic lattice with exact mobility edges,” *Physical Review Letters*, vol. 125, no. 19, p. 196604, 2020.
- [60] T. Wasak, M. Krych, Z. Idziaszek, M. Trippenbach, Y. Avishai, and Y. Band, “Simple model of a feshbach resonance in the strong-coupling regime,” *Physical Review A*, vol. 90, no. 5, p. 052719, 2014.
- [61] S. Will, *From Atom Optics to Quantum Simulation: Interacting Bosons and Fermions in Three-Dimensional Optical Lattice Potentials*. Springer Science & Business Media, 2012.
- [62] J. H. Wilson, Y. Fu, S. D. Sarma, and J. Pixley, “Disorder in twisted bilayer graphene,” *Physical Review Research*, vol. 2, no. 2, p. 023325, 2020.
- [63] H. Yao, T. Giamarchi, and L. Sanchez-Palencia, “Liebliniger bosons in a shallow quasiperiodic potential: Bose glass phase and fractal mott lobes,” *Physical Review Letters*, vol. 125, no. 6, p. 060401, 2020.
- [64] H. Yao, H. Khoudli, L. Bresque, and L. Sanchez-Palencia, “Critical behavior and fractality in shallow one-dimensional quasiperiodic potentials,” *Physical review letters*, vol. 123, no. 7, p. 070405, 2019.